

# IMPROVED GAS BUBBLE MOBILITY IN CHIC-TYPE FLOW CHANNELS

C. Litterst<sup>1</sup>, J. Kohnle<sup>2</sup>, H. Ernst<sup>2</sup>, S. Messner<sup>2</sup>, H. Sandmaier<sup>2</sup>, R. Zengerle<sup>1</sup>, P. Koltay<sup>1</sup>  
<sup>1</sup>IMTEK, University of Freiburg, Freiburg, Germany, <sup>2</sup>HSG-IMIT, Villingen-Schwenningen, Germany

## Abstract:

Recently the authors have presented a unique solution for preventing clogging of microfluidic channels by gas bubbles [1]. It has been shown, that the bubble mobility can be enhanced, if two rectangular channels are nested in a T-shape. This geometrical configuration has been termed channel-in-channel (CHIC) design. In this paper the analytical approach introduced in [1] is enhanced and generalized. The extended approach, presented in this paper considers explicitly the two different equilibrium states of a gas bubble in dependence of the channel geometry and fluid parameters. The presented model allows the prediction of the bubble position and mobility. It is validated by experiments and it is demonstrated how it can be applied to optimise the channel geometry for a given cross section to achieve maximum bubble mobility.

Keywords: microchannel, clogging, bubble, CHIC, capillary driven flow

## Introduction

Since the early days of microfluidics, it is a well-known phenomena that small gas bubbles in capillaries are able to completely block the liquid flow [2]. To handle this problem, gas bubbles have to be removed from the system by bubble traps or guided by appropriate geometrical designs [1], [3]. The CHIC-design shown in Fig. 1 has been found to enhance bubble transport and avoid clogging in capillary systems. It consists of two hydrophilic rectangular channels, forming a T-shaped structure.

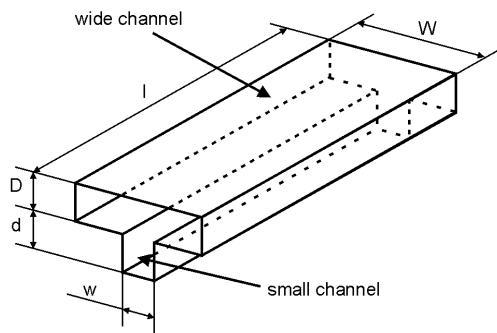


**Fig. 1:** Sketch of a CHIC-type channel geometry (*channel in channel*)

A gas bubble trapped in a CHIC-type channel adopts an equilibrium state which depends on the channels' dimensions and the contact angle  $\Theta$ . In case of a hydrophilic channel the gas bubble can adopt one of two stable states. Both equilibrium states are characterised by the attribute that one part of the channel is left free for liquid flow which then acts as a bypass. Therefore the complete blockage of a channel is reproducibly avoided.

## CFD-simulations

To study the bubble formation inside CHIC-type channels, Computational Fluid Dynamics (CFD) simulations have been performed, using CFDRCs ACE+ package [4]. The initial state for all simulations has been a gas bubble (air) obstructing the complete channels cross section filled with water as depicted in Fig. 2a). For contact angles of  $\Theta \neq 90^\circ$ , the bubble forms into one of two stable states, that depend on the geometrical layout of the channel dimensions  $W$ ,  $w$ ,  $D$  and  $d$  (see Fig. 1). These two states will be referred to as either "horizontal" as depicted in Fig. 2b) or "vertical" like in Fig. 2c). A criterion which state a bubble adopts in a given channel geometry will be given later.

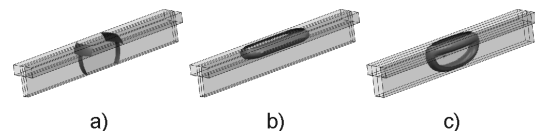


**Fig. 2:** Bubble positions in a CHIC-type channel determined by CFD simulation. a) initial state of the simulation b) final state with a horizontal bubble ( $W = 250$ ,  $w = 31.25$ ,  $D = 100$ ,  $d = 200$  in  $\mu\text{m}$ ) c) final state with a vertical bubble ( $W = 250$ ,  $w = 125$ ,  $D = 100$ ,  $d = 200$  in  $\mu\text{m}$ )

Depending on the contact angle gas bubbles can adopt different stable states. For a contact angle of  $\Theta < 90^\circ$  the bubble forms into a horizontal or vertical position depending on the channel geometry. At a contact angle of close to  $\Theta = 90^\circ$ , the complete channel is blocked, whilst for contact angles of  $\Theta > 90^\circ$  the gas volume moves into a horizontal position with different shape (see Fig. 3). All these statements were proven by simulations.

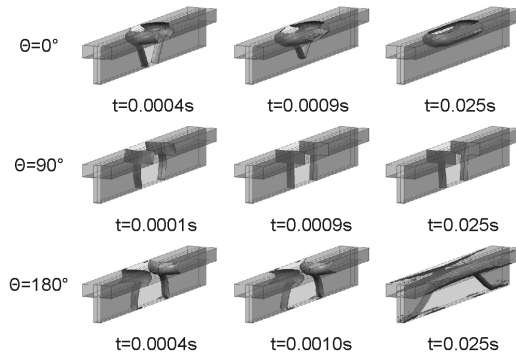


**Fig. 3:** CFD simulation of the relaxation process of a gas bubble initially obstructing both channels ( $W = 250$ ,  $w = 62.5$ ,  $D = 100$ ,  $d = 200$  in  $\mu\text{m}$ ) for different contact angles (media: water and air)

### Analytical modelling

Provided  $\Theta < 90^\circ$  an analytical model can be given which describes the bubble position as function of the geometry parameters ( $W$ ,  $w$ ,  $D$ ,  $d$ ). As the bubble formation is driven by minimization of surface energy, a gas bubble with a given volume  $V$  minimizes its surface area  $A$ . For CHIC-channels one can distinguish between two stable states a bubble can attain (see Fig. 2). These two states do have different surface areas that are  $A_h$  for horizontal bubbles (Fig. 2b)) and  $A_v$  for vertically oriented bubbles (Fig. 2c)). In the analytical model the bubble's surface is approximated by a tetrahedral form and the bubble's length is replaced by the ratio of the bubble volume  $V$  divided by the bubble's width and depth. Thus the surface areas of the two bubble positions yield:

$$A_h = 2 * \left( W * D + \frac{V}{W * D} (W + D) \right) \quad (1)$$

$$A_v = 2 * \left( w * (D + d) + \frac{V * (w + D + d)}{w * (D + d)} \right) \quad (2)$$

Both equations consist of a term describing the bubble cap areas and a term describing the bubble's shell in dependence of the bubble's length. The contribution of the bubble cap areas are  $W * D$  and  $w * (D + d)$  respectively. If it is assumed, that the gas bubble's length is large against its cross-sectional dimensions, it follows that the surface area of the bubble's shell is dominant against the bubble cap area. These contributions become even more negligible if the total surface areas of the vertical and the horizontal position are compared to each other. The total shell areas can be compared to each other by setting the bubble volume to unity. This

yields to the following criterion for equal bubble surfaces  $A_h \approx A_v$ :

$$\frac{D + W}{D * W} \approx \frac{D + d + w}{w * (D + d)} \quad (3)$$

This equation defines a separation line between the two regimes. From this the attained bubble position can be deduced directly: If the volume of the horizontal bubble is smaller ( $A_h < A_v$ ), a horizontal position is attained. In opposite, for  $A_h > A_v$  the vertical bubble position is preferred to minimize the bubble surface. In reality a discrete crossover between the two states - like implied in equation (3) - is not observed. Experiments show the existence of a certain crossover region where none of the two positions is adopted and the shape of the bubble depends on details of the geometry like surface roughness, tolerances, etc. For geometries within this crossover region unstable bubble positions or complete blocked channels are observed (cf. Fig. 4).

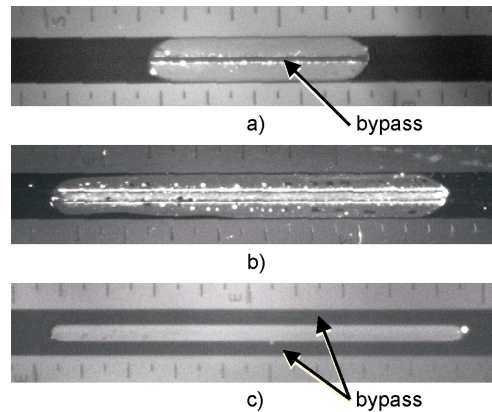


**Fig. 4:** Top view photographs of the different bubble configurations inside test channels (media: coloured water and air) with a) horizontal, b) blocked and c) vertical bubble position. The photos a) to c) correspond to the sketches of Fig. 6 d) to f).

With this criterion for the bubble position it is now possible to extend the model for the mobility of gas bubbles in CHIC-channels presented in [1]. We consider the rise velocity of a bubble in a CHIC channel subjected to buoyant forces in a vertically arranged experimental setup with sealed channel ports. The rise velocity of the bubble can be determined by comparing the upward directed gas flow rate  $\Phi_{\text{gas}}$  and the downward vectored liquid flow rate  $\Phi_{\text{liq}}$ . Following [1] the maximum velocity is given by equating both flow rates. Hereby the gas flow rate is defined as the rise velocity of the bubble divided by its cross-section area. The liquid flow rate is defined as the hydrostatic pressure difference over the bubbles length divided by the fluidic

resistance of the liquid filled channel part. Due to the different bubble positions both flow rates have to be defined case sensitive for either the horizontal or the vertical bubble position. In the case of the horizontal bubble the maximum velocity reads as already shown in [1]:

$$\bar{v}_h = \frac{\rho * g * w^3 * d^3}{8 * \eta * (w + d)^2 * W * D} \quad (4)$$

The velocity for the vertical bubble position can be deduced in the same way. The difference is only given through the different channel parts occupied either by liquid or gas in the two different cases. In case of the vertical bubble position two bypasses are formed (cf. Fig. 4c)). The two liquid filled channels left and right of the bubble are treated as a parallel connection of two fluidic resistances in the calculation. This yields an analytical maximum velocity for vertical bubbles of:

$$\bar{v}_v = \frac{\rho * g * D^3 * (W - w)^3}{8 * \eta * w * (D + d) * (2 * D + W - w)^2} \quad (5)$$

In this model for the rise velocity the effective length of the gas bubble  $l_{\text{bub}}$ , the bubble volume  $V$ , the contact angle  $\Theta$  and the wall friction are not considered. Thus the equation can only be used to estimate the maximum bubble velocity for ideal channels in the limit of “large” bubble lengths. For “short” bubbles other effects like slip-stick might dominate and the velocity is generally dependent on the bubble volume. In experiments generally a saturation of the velocity is observed with increasing bubble length (cf.[1], [5])

Instead of the velocity  $\bar{v}$  the bubble mobility  $b$  might be considered which for the vertical case is defined as:

$$b = \frac{\text{velocity}}{\text{pressure difference}} = \frac{\bar{v}}{\rho * g * l_{\text{bub}}} \quad (6)$$

Setting the bubble length to unity and using the criterion for the bubble position inside a channel given by equation (3), the bubble mobility can be displayed in a 3-dimensional plot as depicted in Fig. 5. In this chart the geometrical parameters  $w$  and  $d$  are varied, while the overall cross section of the channel is kept constant at a value of  $(W + w) * (D + d) = 1000 * 300 \mu\text{m}^2$ . The maximum mobility for the gas bubbles is theoretically achieved for the situation where  $A_h = A_v$ , but in practice never attained due to the existing crossover region mentioned before. The theoretical absolute maximum for the considered case calculates to  $b = 2.437 \mu\text{m Pa}^{-1} \text{s}^{-1}$  and is reached for the channel

geometry characterized by  $W = 1000 \mu\text{m}$ ,  $w = 248 \mu\text{m}$ ,  $D = 157.1 \mu\text{m}$  and  $d = 142.9 \mu\text{m}$  for a vertical bubble configuration. The highest velocities are reached on the right side of the separation line which forms a ridge in the displayed surface. For many configurations along this ridge the model predicts an at least one order of magnitude larger bubble mobility for vertical bubbles than for horizontal ones.

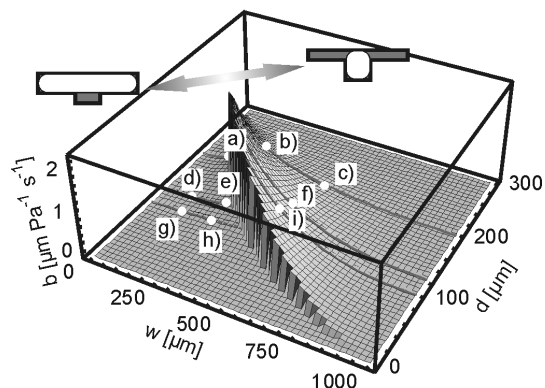


**Fig. 5:** Maximum theoretical mobility  $b$  of gas bubbles in CHIC-channels as function of  $d$  and  $w$  at a fixed value of  $W = 1000 \mu\text{m}$  and total depth  $D + d = 300 \mu\text{m}$ . The parameter sets depicted in Fig. 6 a) to i) are displayed as dots and refer to the realized test samples.

### Experimental model verification

To verify the analytical model, the first check that had been done was to investigate if the bubble position inside the channel is predicted correctly by equation (3). The media used for all presented experiments has been deionised, coloured water and air. The test samples used for experiments have been realized by deep reactive ion etching in silicon and were sealed with a Pyrex cover by anodic bonding. Different geometries were realized as depicted in Fig. 5.

Since the approximation of the bubble surface by a tetrahedral skin is relatively crude, the evidence of this part of the model was of particular importance. However the proposed criterion turned out to give reliable results as displayed in Fig. 6, where the bubble position attained in experiments is sketched qualitatively. Except for the channels a) and e) all positions are predicted correctly. The reason for failure of the model in case a) and e) is their closeness to the crossover region.

As stated before, the equilibrium bubble position for similar surface areas  $A_h \approx A_v$  is very sensitive to the microscopic details of the structure like surface roughness etc. and often even not very stable. In most cases a complete blockage of the channel is

observed. Therefore the model is deemed to fail close to the separation line given by equation (3) in the so termed crossover region. Due to the limited number of the available test-samples, the width of this crossover region could not be determined yet.

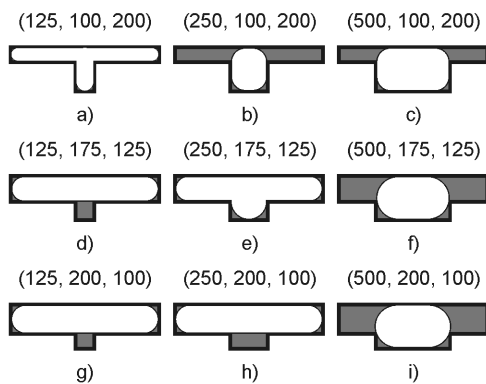


**Fig. 6:** Qualitative sketches of the equilibrium bubble position obtained by experiments. The numbers in brackets signify  $w$ ,  $D$  and  $d$  in  $\mu\text{m}$  respectively ( $W = 1000 \mu\text{m}$ )

The second part of the model which predicts the buoyant velocity has been verified by comparing the maximum attainable velocities in the test channels by the predicted maximum value. The results of these buoyancy experiments are summarized in Fig. 7 with the bubble mobilities. The mobilities obtained in channels c), d) and g) showed a very good agreement with the analytical model and always stayed below the predicted values. This fact is important, as the assumptions made for the analytical model are for ideal channels. In the case of channel h) the predicted maximum mobility was not reached because the bubble showed a stick-slip behaviour and therefore was much slower than anticipated. The channel a) and e) were completely blocked because of being too close to the separation line and therefore exhibited poor mobility. Due to the fact, that the channels realized in the test samples had a maximal length of 70 mm, the maximum attainable mobility was not reached in all channels. For the channels i), b) and f) the available channel length was too short to reach saturation of the mobility. It remains to be shown, that longer bubbles than 70 mm can reach the predicted mobilities in these channel types.

Although the maximum predicted mobility could not be experimentally confirmed for all channels with vertical bubble positions, the actually measured values for the vertical bubbles are about one order of magnitude higher than for the horizontal bubbles. Thus they have to be considered as advantageous for degassing microfluidic channels and for preventing clogging.

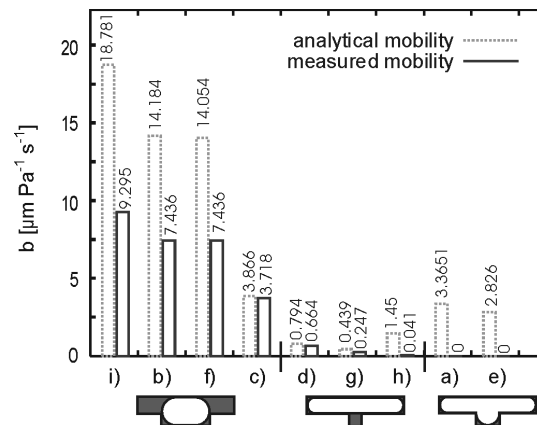


**Fig. 7:** Measured maximum buoyant mobilities of gas bubbles ( $l_{\text{bub}} = 55 \text{ mm}$ ) for the various configurations shown in Fig. 6 and in comparison the analytically predicted mobilities.

## Conclusions

After having discussed in detail the bubble dynamics in CHIC-channels it can be concluded, that vertical gas bubbles have much higher mobilities than horizontal ones in hydrophilic channels ( $\Theta < 90^\circ$ ). Therefore vertical bubbles are better suited for removing gas from microfluidic systems. With the proposed analytical model one can predict in which cases this favourable bubble position is obtained and which maximum mobility can be expected.

Due to the approximations made in deriving the analytical model following restrictions need to be taken into account: 1. Channel designs where a horizontal bubble and a vertical bubble would have a similar surface area (i.e. parameter sets within the crossover region) cannot be treated properly. 2. The predicted mobility is only attained for sufficiently long bubbles, when the buoyant velocity has saturated. In practice smaller values might occur.

## References

- [1] J. Kohnle et al., A Unique Solution for Preventing Clogging of Flow Channels by Gas Bubbles, Proc. MEMS 2002, 77 – 80
- [2] P. Gravesen et al., Microfluidics – A Review, J. Micromech. Microeng. 3 (1993), 168 – 182
- [3] M. Jensen et al., Dynamics of Bubbles in Microchannels, microTAS 2002, 2, 733 – 735
- [4] H. Yang, A. Przekwas, Computational Modeling of Microfluid Devices with Free Surface Liquid, Proc. MSM 1998, 498 - 505
- [5] E. White, R. Beardmore, The Velocity of Rise of Single Cylindrical Air Bubbles Through Liquids Contained in Vertical Tubes, Chem. Eng. Sci., 1962, Vol. 17, 351 - 361